

# Dynamic FT-IR Analysis of the Crystallization to the Planar Zigzag Form for Syndiotactic Polypropylene

Takahiko Nakaoki\* and Tetsushi Yamanaka

Department of Materials Chemistry, Ryukoku University, Seta, Otsu 520-2194, Japan

Yasumasa Ohira and Fumitaka Horii\*

Institute for Chemical Research, Kyoto University, Uji, Kyoto 611-0011, Japan

Received September 10, 1999; Revised Manuscript Received January 3, 2000

**ABSTRACT:** The polymorph and crystallization process for syndiotactic polypropylene (sPP) formed around at 0 °C after quenching from the melt has been dynamically investigated by infrared spectroscopy. The observation is carried out at constant temperatures between –5 and 15 °C after quenching into ice–water from the melt. Just after quenching into ice–water from the melt, the specimen is completely in the noncrystalline state with trans-rich sequences. When the samples are kept below 0 °C, only the planar zigzag form (form III) is crystallized in a few hours. Above 5 °C, in addition to the planar zigzag form, form I with the  $t_2g_2$  conformation is simultaneously formed. Just above the glass transition temperature (around –5 °C), the trans-rich chains are aggregated and developed to form form III. Above 5 °C, the trans–gauche transition is accelerated, and then the helical form with  $t_2g_2$  conformation is crystallized as form I. The total degree of crystallinity is not so high, because further crystallization is promoted in the noncrystalline region when the sample is left at room temperature after reaching the equilibrium state at each crystallization temperature.

## Introduction

It has been established that syndiotactic polypropylene (sPP) shows polymorphism depending on crystallization conditions. Synthesis of high stereoregular samples of syndiotactic polypropylene by recent improvements of catalysts enables the determination of a more accurate crystal structure.<sup>1</sup> As for the crystal modifications, there are four types of crystal structures with different conformations and unit cells. According to the nomenclature of Corradini et al.,<sup>2</sup> two forms with the  $t_2g_2$  conformation are termed form I and form II while the modifications with the planar zigzag and  $t_2g_2t_6g_2$  sequences are termed form III and form IV, respectively. The former two modifications are known to take on the most stable conformation.<sup>3–14</sup> A conventional method for crystallization to form III with the planar zigzag form required the cold-drawing process.<sup>15–18</sup> However, we recently reported that this conformational form could be obtained by holding in ice–water for several hours after quenching into ice–water from the melt.<sup>19</sup> It is worth noting that this process needs no elongation process. Our previous research<sup>19</sup> was performed at room temperature by solid-state high-resolution  $^{13}\text{C}$  NMR and wide-angle X-ray diffraction methods. The contribution due to form I with the  $t_2g_2$  conformation in addition to form III was also observed. Therefore, the purpose of the present work is to elucidate the relationship between the crystallization processes of form III and form I at different temperatures around 0 °C. Very recently, a similar investigation was also performed for the spontaneous crystallization of form III at 0 °C by real-time wide-angle X-ray diffraction and high-resolution solid-state  $^{13}\text{C}$  NMR methods. The results will be reported in our recent paper.<sup>20</sup>

Infrared spectroscopy is a powerful method to investigate real time changes in molecular structure as time-resolved processes. Vibrational modes are quite sensitive to molecular symmetry so that the different

conformations are directly reflected in the spectrum. The vibrational frequencies for the  $t_2g_2$  and planar zigzag conformations were calculated by using a valence force field.<sup>21</sup> The characteristic bands of each form were reported by Tadokoro et al.<sup>16</sup>

In this paper, we deal with the polymorphs and the crystallization process around 0 °C for the sPP sample quenched from the melt. To make the dynamic process clear, time-resolved infrared spectral measurements are carried out at various temperatures.

## Experimental Section

**Sample.** The sPP sample was supplied from Mitsui Chemical Co. Ltd. The molecular weight ( $M_w$ ) and racemic pentad contents (rrrr) were  $1.55 \times 10^5$  and 0.96, respectively.

**FT-IR Measurements.** Infrared spectra were measured by a JASCO FT-IR 8300 instrument equipped with a DTGS detector with a resolution of 2  $\text{cm}^{-1}$ . For each spectrum 8 or 16 transients were collected. A sample chamber kept at a constant temperature was made by our laboratory. The temperature was controlled within  $\pm 0.5$  °C. The films for infrared measurements were prepared as follows. A thin sPP film about 20  $\mu\text{m}$  thick was prepared in a molding press at 170 °C. It was wrapped by an aluminum foil and placed between two thin metal plates. This sample was immersed into a glycerine bath at 170 °C for 30 min and then quenched into ice–water. For isothermal infrared measurements, the film was quickly taken out of the aluminum foil in a globe box kept at 0 °C and moved to the sample chamber of the FT-IR spectrometer kept at a constant temperature.

## Results and Discussion

**Isothermal Crystallization Process.** Our previous CP/MAS  $^{13}\text{C}$  NMR measurements for the crystallization of form III of sPP were carried out by using the film that was kept at room temperature overnight after quenched into ice–water.<sup>19</sup> Figure 1 shows infrared spectra of the specimens prepared under the same crystallization conditions as our previous report.<sup>19</sup> The

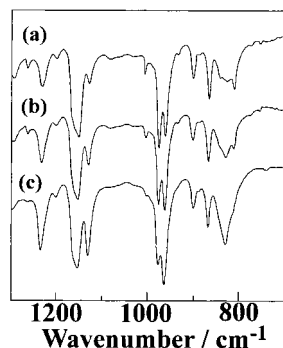


**Figure 1.** Infrared spectra measured at room temperature for the sPP films which were quenched into ice–water from the melt and kept there for different periods: (a) 5 min, (b) 1 h, and (c) 24 h.

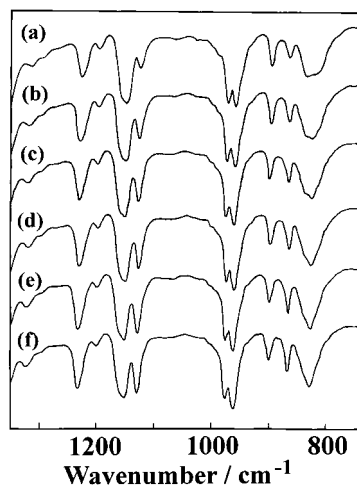


**Figure 2.** Time dependence of infrared spectra measured at 0 °C for the sPP film quenched into ice–water from the melt: (a) 5 min, (b) 30 min, (c) 45 min, (d) 1 h, (e) 5 h, and (f) 10 h.

spectrum for the film kept in ice–water for 5 min is characterized by the peaks of 812, 842, 977, 1005, and 1264  $\text{cm}^{-1}$ , which are assignable to form I with the  $t_2g_2$  conformation. Both form I and form II take the same  $t_2g_2$  conformation but with different unit cells. Although it is difficult to distinguish these crystal modifications due to the different chain packings using infrared spectra, the formation of form I under this condition was confirmed by the previous wide-angle X-ray diffractometry.<sup>19,20</sup> When the samples are kept at 0 °C for 1 h, these characteristic peaks decrease remarkably in intensity.

In contrast, the spectral profile after 20 h is featured by the peaks of 829, 963, 1130, and 1230  $\text{cm}^{-1}$ . These modes are attributed to the planar zigzag form, form III. This leads to the same conclusion previously reported by high-resolution solid-state  $^{13}\text{C}$  NMR and X-ray diffraction methods that form III is spontaneously produced at 0 °C in several hours.<sup>19,20</sup> However, even after 20 h, a small amount of form I with the  $t_2g_2$  conformation is observed in the spectrum. Annealing at room temperature is suggested to be a very important factor to induce the crystallization of form I.

To eliminate the annealing effect at room temperature, the infrared spectra have been measured at 0 °C after quenching into ice–water from the melt without increasing the sample temperature above 0 °C. The result is shown in Figure 2. Just after quenching to 0 °C from the melt as shown in Figure 2a, most of the

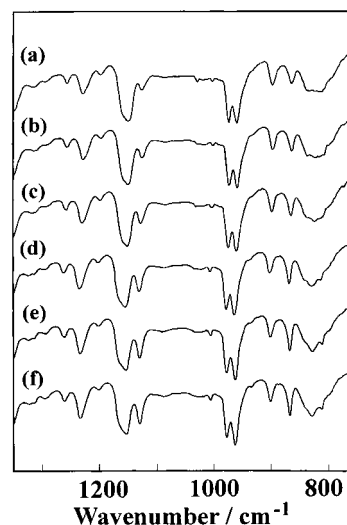
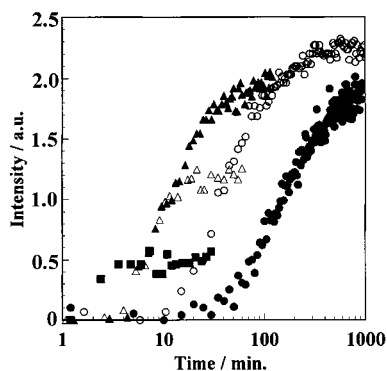


**Figure 3.** Time dependence of infrared spectra measured at 10 °C for the sPP film quenched into ice–water from the melt: (a) 1 min, (b) 4 min, (c) 6 min, (d) 9 min, (e) 30 min, and (f) 60 min.

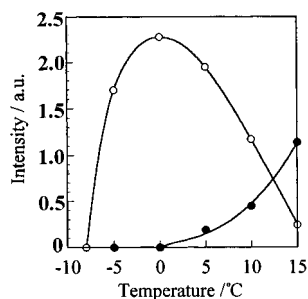
peaks provide broad profiles, and there is no characteristic band due to ordered conformations such as the planar zigzag and  $t_2g_2$  conformations. This fact indicates that the film is in the noncrystalline state. With increasing time, the peaks at 829, 963, and 1130  $\text{cm}^{-1}$  increase in intensity. These modes are attributed to form III with the planar zigzag form as described above. It is worth noting that vibrational modes due to the  $t_2g_2$  conformation cannot be observed. This indicates that the conformational arrangement at 0 °C is restricted to induce only the planar zigzag form, in good accord with the results previously obtained by WAXS and CP/MAS  $^{13}\text{C}$  NMR measurements.<sup>19,20</sup> Here, a question remains unanswered as to how the temperature relates to the crystallization processes for form III and form I.

Figure 3 shows the spectral change for the sample held at 10 °C just after being quenched at 0 °C. First, no characteristic band for the ordered structures is observed. With increasing time, in addition to the increment of peak intensity due to form III, the bands due to the  $t_2g_2$  conformation increase in intensity. This phenomenon can be interpreted by the simultaneous crystallization of form III and form I or form IV with the  $t_2g_2t_6g_2$  conformation proposed by Chatani et al.<sup>22</sup> According to our previous analysis by high-resolution solid-state  $^{13}\text{C}$  NMR spectroscopy,<sup>19</sup> the resonance line at 44 ppm assigned to the methylene carbon with one  $\gamma$ -gauche effect is very weak and broad for the sample prepared under the same conditions as for the infrared measurements. Therefore, form IV containing the methylene carbon with one  $\gamma$ -gauche effect is not produced, but form I with the  $t_2g_2$  conformation is isothermally formed. This fact supports the conclusion that both crystallizations of form III and form I are simultaneously induced. After 1 h, the spectral profile reaches an almost stationary state as seen in Figure 3f.

To quantitatively characterize these processes, the bands assigned to the rocking mode of the main chain methylene have been selected because the sharp peaks of form III and form I are separately observed at 829 and 812  $\text{cm}^{-1}$ , respectively. In Figure 4, the absorbance at 829  $\text{cm}^{-1}$  is plotted against crystallization time at different temperatures for the sample quenched in ice–water. Here, the 3220  $\text{cm}^{-1}$  band, which may be ascribed



**Figure 4.** Time change in absorbance intensity for the 829  $\text{cm}^{-1}$  band assigned to form III with the planar zigzag conformation at various temperatures: (●)  $-5\text{ }^{\circ}\text{C}$ , (○)  $0\text{ }^{\circ}\text{C}$ , (▲)  $5\text{ }^{\circ}\text{C}$ , (△)  $10\text{ }^{\circ}\text{C}$ , and (■)  $15\text{ }^{\circ}\text{C}$ . The absorbance was normalized by the  $3220\text{ cm}^{-1}$  band as an internal standard.



**Figure 5.** Temperature dependence of the level-off absorbance intensity for different polymorphs: (○) form III, (●) form I.

to the combination mode of lower frequency modes, is used as an internal reference to calibrate the film thickness, because this band is comparatively isolated with other modes, and there is no remarkable change in intensity during the measurements. The stationary level of the intensity of the  $829\text{ cm}^{-1}$  band observed after a long period corresponds to the highest degree of crystallinity at that temperature. The level-off intensities at the respective temperatures are plotted as shown in Figure 5. The crystallinity of form III gives a maximum level at  $0\text{ }^{\circ}\text{C}$ . When the sample is kept at  $-8\text{ }^{\circ}\text{C}$ , the infrared spectrum shows no characteristic bands associated with ordered crystalline structures even after 72 h. As the glass transition temperature ( $T_g$ ) for sPP is about  $-5\text{ }^{\circ}\text{C}$ ,<sup>20</sup> the molecular motion is frozen at  $-8\text{ }^{\circ}\text{C}$ , and as a result the crystallization is completely hindered. Above  $0\text{ }^{\circ}\text{C}$ , the content of form III decreases successively with increasing temperature. In Figure 5, the peak at  $812\text{ cm}^{-1}$  due to form I is also plotted. Above  $5\text{ }^{\circ}\text{C}$ , the peak intensity increases.

The crystallization mechanism will be explained as follows: Just after quenching in ice–water from the melt, the sample is completely in the noncrystalline state, but the local sequences predominately adopt trans conformations.<sup>20</sup> Above  $T_g$ , the aggregation among the molecular chains with the trans-rich sequences constructs the crystals of form III. The development of trans–gauche transitions with increasing temperature may allow the molecular chains to take the  $t_2g_2$  helical conformation. As a result, above  $0\text{ }^{\circ}\text{C}$  the molecular chains with the  $t_2g_2$  conformation are packed as crystals of form I.

**Annealing Effects at Room Temperature for Samples Kept at 0 and  $10\text{ }^{\circ}\text{C}$ .** Judging from the result shown in Figure 4, the crystallization seems to almost

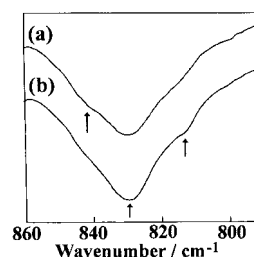


**Figure 6.** Infrared spectra for the methylene rocking mode: (a) measured at  $0\text{ }^{\circ}\text{C}$  for the sPP film kept at  $0\text{ }^{\circ}\text{C}$  for 24 h; (b) measured at room temperature for the same sample after further left at room temperature overnight.

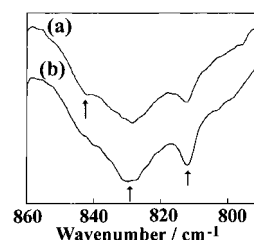


**Figure 7.** Infrared spectra for the methylene rocking mode: (a) measured at  $10\text{ }^{\circ}\text{C}$  for the sPP film kept at  $0\text{ }^{\circ}\text{C}$  for 24 h; (b) measured at room temperature for the same sample after further left at room temperature overnight.

finish within a few hours at each temperature. However, further crystallization was confirmed when the sample was taken out of the apparatus and left at room temperature. After measured at  $0\text{ }^{\circ}\text{C}$  for 24 h as shown in Figure 2, the film was left at room temperature overnight, and then the infrared spectrum was observed for this film. In Figure 6, the infrared spectral profiles of the methylene rocking mode before and after being left at room temperature are shown. The noncrystalline component around  $842\text{ cm}^{-1}$  disappears, and alternatively the peaks at  $812\text{ cm}^{-1}$  due to form I clearly increase in intensity. In addition, the contribution from form III appearing at  $829\text{ cm}^{-1}$  also becomes large. This result indicates further crystallization of form III and a newly forming process of form I, in good accord with the previous observation by high-resolution solid-state  $^{13}\text{C}$  NMR and wide-angle X-ray diffraction methods.<sup>20</sup> Figure 7 shows a similar case measured at room temperature after being kept at  $10\text{ }^{\circ}\text{C}$ . Similarly, the decrease in intensity at  $842\text{ cm}^{-1}$  and the increases in intensity at  $812$  and  $829\text{ cm}^{-1}$  are observed. This fact corresponds to the simultaneous crystallization growth of form III and form I. These results suggest that the degree of crystallinity formed around  $0\text{ }^{\circ}\text{C}$  is not so high at the respective temperatures.

To obtain further information on the crystallization process at room temperature, the time change in infrared spectrum for the sample left at room temperature after quenched in ice–water was measured. Figure 8 shows the spectral change at room temperature for the film after kept in ice–water for 5 min. The period kept at  $0\text{ }^{\circ}\text{C}$  is too short to yield form III, so that Figure 8a features the noncrystalline state. With increasing time, both bands for form III and form I increase in intensity. Figure 9 shows the time change of the absorbance for both bands. In addition, the values for the noncrystalline component at  $842\text{ cm}^{-1}$  are also plotted. Contrary to the increment in intensity for crystalline forms of form III and form I, the absorbance for the noncrystalline state decreases in intensity. This shows that both crystal forms are simultaneously

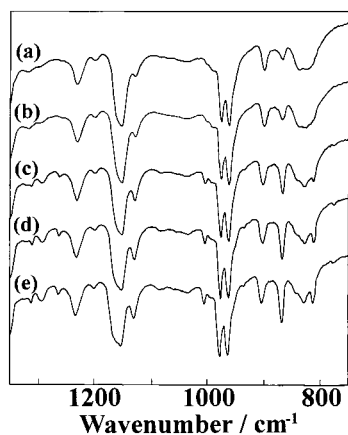


**Figure 8.** Time change of infrared spectra measured at room temperature for the sPP film just after kept at 0 °C for 5 min: (a) 0.63 min, (b) 1.5 min, (c) 2.5 min, (d) 5.5 min, and (e) 45 min.

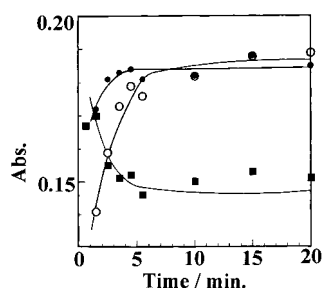


**Figure 9.** Time dependence of the absorbance intensity for different components appearing in the sPP film that is shown in Figure 8: (○) form III, (●) form I, and (■) noncrystalline component.

crystallized in the noncrystalline region. The crystallization around 0 °C is not enough to reach a high degree of crystallinity. It remains in the noncrystalline state in a significantly wide region even after several tens of hours. When the sample is left at room temperature, the rapid crystallization, that is the aggregation among trans-rich chains and the crystallization due to the enhancement of trans-gauche transitions, occurs in the noncrystalline region.

## Conclusion

Dynamical FT-IR measurements around 0 °C have revealed the crystallization processes of form III and form I from the melt. Just after quenched into ice-water from the melt, the sPP sample is in the noncrystalline

state. Below 0 °C, only form III is crystallized from the noncrystalline state. However, the degree of crystallinity is not so high, because this form is further produced when the sample is left at room temperature. When the sample is kept above 5 °C after quenched at 0 °C from the melt, both crystallizations to form III and form I are simultaneously induced. Similarly to the cases observed below 0 °C, further crystallizations occur when the temperature is increased to room temperature. The extent of the trans-gauche transition will be one of possible important factors to control the formation of the crystals of sPP with characteristic conformations at a given temperature around 0 °C.

## References and Notes

- (1) Ewen, J. A.; Jones, R. L.; Razavi, A.; Ferrara, J. D. *J. Am. Chem. Soc.* **1988**, *110*, 6255.
- (2) De Rosa, C.; Auriemma, F.; Corradini, P. *Macromolecules* **1996**, *29*, 7452.
- (3) Lotz, B.; Lovinger, A. J.; Cais, R. E. *Macromolecules* **1988**, *21*, 2375.
- (4) Lovinger, A. J.; Lotz, B.; Davis, D. D. *Polymer* **1990**, *31*, 2253.
- (5) Lovinger, A. J.; Davis, D. D.; Lotz, B. *Macromolecules* **1991**, *24*, 552.
- (6) Lovinger, A. J.; Lotz, B.; Davis, D. D.; Padden, F. J. *Macromolecules* **1993**, *26*, 3494.
- (7) De Rosa, C.; Corradini, P. *Macromolecules* **1993**, *26*, 5711.
- (8) Auriemma, F.; De Rosa, C.; Corradini, P. *Macromolecules* **1993**, *26*, 5719.
- (9) Sozzani, P.; Simonutti, R.; Galimberti, M. *Macromolecules* **1993**, *26*, 5782.
- (10) Lovinger, A. J.; Lotz, B.; Davis, D. D.; Schumacher, M. *Macromolecules* **1994**, *27*, 6603.
- (11) Auriemma, F.; Born, R.; Spiess, H. W.; De Rosa, C.; Corradini, P. *Macromolecules* **1995**, *28*, 6902.
- (12) Auriemma, F.; Lewis, R. H.; Spiess, H. W.; De Rosa, C. *Macromol. Chem.* **1995**, *196*, 4011.
- (13) Auriemma, F.; Born, R.; Spiess, H. W.; De Rosa, C.; Corradini, P. *Macromolecules* **1995**, *28*, 6902.
- (14) De Rosa, C.; Auriemma, F.; Vinti, V. *Macromolecules* **1997**, *30*, 4137.
- (15) Natta, G.; Peraldo, M.; Allegra, G. *Makromol. Chem.* **1964**, *75*, 215.
- (16) Tadokoro, H.; Kobayashi, M.; Kobayashi, S.; Yasuhuku, K.; Mori, K. *Rep. Prog. Polym. Phys. Jpn.* **1966**, *9*, 181.
- (17) Chatani, Y.; Maruyama, H.; Noguchi, K.; Asanuma, T.; Shiomura, T. *J. Polym. Sci., Polym. Phys. Lett.* **1990**, *28*, 393.
- (18) Sozzani, P.; Galimberti, M.; Balbontin, G. *Makromol. Chem. Rapid Commun.* **1993**, *13*, 305.
- (19) Nakaoki, T.; Ohira, Y.; Hayashi, H.; Horii, F. *Macromolecules* **1998**, *31*, 2705.
- (20) Ohira, Y.; Horii, F.; Nakaoki, T., submitted to *Macromolecules*.
- (21) Schachtschneider, J. H.; Snyder, R. G. *Spectrochim. Acta* **1965**, *21*, 1527.
- (22) Chatani, Y.; Maruyama, H.; Asanuma, T.; Shiomura, T. *J. Polym. Sci., Polym. Phys. Ed.* **1991**, *29*, 1649.

MA9915428